Journal of Integrative Neuroscience

*J. Integr. Neurosci.* **2022**; 21(3): 88
https://doi.org/10.31083/j.jin2103088

*Original Research*

# Alterations in somatosensory, visual and auditory pathways in amyotrophic lateral sclerosis: an under-recognised facet of ALS

Rangariroyashe H. Chipika[1,†], Grainne Mulkerrin[1,†], Aizuri Murad[1], Jasmin Lope[1], Orla Hardiman[1], Peter Bede[1,2,*]

[1]Computational Neuroimaging Group, Trinity College Dublin, D02 R590 Dublin, Ireland
[2]Department of Neurology, St James's Hospital, D08 NHY1 Dublin, Ireland
*Correspondence: bedep@tcd.ie (Peter Bede)
[†]These authors contributed equally.

Academic Editors: Foteini Christidi and Efstratios Karavasilis
Submitted: 2 December 2021 Revised: 30 December 2021 Accepted: 7 January 2022 Published: 27 April 2022

**Abstract**

**Background**: While amyotrophic lateral sclerosis (ALS) is widely recognised as a multi-network disorder with extensive frontotemporal and cerebellar involvement, sensory dysfunction is relatively under evaluated. Subtle sensory deficits have been sporadically reported, but there is a prevailing notion that sensory pathways may be relatively spared in ALS. **Methods**: In a prospective neuroimaging study we have systematically evaluated cerebral grey and white matter structures involved in the processing, relaying and mediation of sensory information. Twenty two *C9orf72* positive ALS patients (C9+ ALS), 138 *C9orf72* negative ALS patients (C9- ALS) and 127 healthy controls were included. **Results**: Widespread cortical alterations were observed in C9+ ALS including both primary and secondary somatosensory regions. In C9- ALS, cortical thickness reductions were observed in the postcentral gyrus. Thalamic nuclei relaying somatosensory information as well as the medial and lateral geniculate nuclei exhibited volume reductions. Diffusivity indices revealed posterior thalamic radiation pathology and a trend of left medial lemniscus degeneration was also observed in C9- ALS ($p = 0.054$). Our radiology data confirm the degeneration of somatosensory, visual and auditory pathways in ALS, which is more marked in GGGGCC hexanucleotide repeat expansion carriers. **Conclusions**: In contrast to the overwhelming focus on motor system degeneration and frontotemporal dysfunction in recent research studies, our findings confirm that sensory circuits are also affected in ALS. The involvement of somatosensory, auditory and visual pathways in ALS may have important clinical ramifications which are easily overlooked in the context of unremitting motor decline. Subtle sensory deficits may exacerbate mobility, contribute to fall risk, impair dexterity, and worsen bulbar dysfunction, therefore comprehensive sensory testing should also be performed as part of the clinical assessments in ALS.

**Keywords:** Amyotrophic lateral sclerosis; Motor neuron disease; Sensory pathways; Neuroimaging; MRI

## 1. Introduction

### *1.1 Background*

Amyotrophic lateral sclerosis (ALS) is a neurodegenerative disease which is primarily characterized by the degeneration of upper and lower motor neurons [1,2]. While frontotemporal pathology is often observed [3], sensory neuropathy, dorsal root ganglion pathology and the degeneration of brain structures involved in sensory processing are not recognised as core features of the disease. Nonetheless, sensory involvement has been observed clinically [4–7], and demonstrated by electrophysiology [4,8–11], neuroimaging [9,12,13] and neuropathology studies [4,14–17]. Sensory dysfunction is thought to be more common in familial ALS than in sporadic ALS [1,18], and sensory disturbances have also been observed in other motor neuron disease phenotypes [19–22]. The literature of sensory dysfunction in ALS is conflicting; most studies report negative findings [23–25], but few studies have evaluated sensory regions specifically [9]. Clinically, subtle paraesthesia [5,26–28], numbness [2], pain [29], vestibular symptoms [30], proprioceptive deficits [31], changes in olfaction [32–34] and taste [35,36] may be overshadowed by progressive limb weakness and bulbar dysfunction [37]. It is noteworthy, that Riluzole, the first FDA approved for the treatment of ALS has been associated with mild circumoral paresthesia [38] but this is rarely a cause for discontinuation. Sensory changes have also been observed in the larynx on fibre-optic endoscopic evaluation of swallowing with sensory testing (FEEST) [39,40].

The substrate of sensory symptoms is most commonly studied by electrophysiology or post mortem, and it is seldom specifically evaluated on neuroimaging [41]. Alterations in sensory nerve action potentials (SNAP) [11,42], somatosensory evoked potentials (SEP) [8,43–46], visual evoked potentials (VEP) [47,48], auditory evoked potentials [8,48] and sensory action potential amplitudes (SAPA) [49] have been sporadically described. There are inconsistent reports on the impairments of thermal sensory pathways, but study protocols differ considerably [24,50]. Overt visual deficits are rarely reported by patients, but impaired visuospatial function has been consistently demonstrated in ALS [51,52]. Microscopically, dorsal root gan-

glion, dorsal column, thalamus, sensory cortex and sensory nerve degeneration has also been observed [25,53,54]. Occipital lobe pathology has been noted in both familial and sporadic ALS patients [55] and occipital pTDP-43 pathology has also been described [56]. On neuroimaging, dorsal column degeneration [9,57,58], thalamic pathology [59,60] and postcentral gyrus [61,62] atrophy have consistently been reported. Structural [63], diffusion [64], functional [65], susceptibility [66], and MR spectroscopy [67] have all captured some degree of parietal and occipital lobe involvement. Despite these reports, there is a prevailing notion that ALS spares sensory networks [68], and no dedicated cerebral studies have systematically investigated the cortical, subcortical and white matter components of sensory pathways.

### *1.2 Objectives, aims and hypotheses*

The primary objective of this study is the systematic evaluation of cortical, subcortical and white matter structures involved in the processing, relaying and mediation of sensory information. Accordingly, a comprehensive panel of cerebral structures was defined associated with specific somatosensory, visual and auditory processes (Table 1). Some of the selected regions such as the postcentral gyrus, the ventral posterolateral (VPL), ventromedial (VM), lateral geniculate (LGN) and medial geniculate (MGN) nuclei of the thalamus and the medial lemniscus are either exclusively or primarily involved in sensory functions. Other regions included in the panel, such as the insular cortex, supramarginal gyrus, superior temporal gyrus, and the posterior thalamic radiation mediate a combination of sensory and non-sensory functions. We hypothesised that cerebral structures involved in somatosensory processes are not spared in ALS. Direct clinico-radiological correlations were not sought, as peripheral and spinal components of sensory pathways were not evaluated in this study [9,69].

## 2. Methods

### *2.1 Participants*

A total of 287 participants, 160 patients with ALS ('ALS') 127 healthy controls ('HC') were included in a prospective, single-centre imaging study. All participants provided informed consent as required by the Ethics Approval of this research project (Beaumont Hospital, Dublin, Ireland). Exclusion criteria included a history of traumatic brain injury, cerebrovascular events, neoplastic, paraneoplastic and neuroinflammatory diagnoses. A total of 7 patients were excluded after enrolment because of incidental radiological findings. Patients with ALS were diagnosed according to the revised El Escorial criteria. Key demographic and clinical variables (ALSFRS-r) were recorded for all participants at the time of their scan and a dedicated sensory assessment was performed in a subset of *C9orf72* negative patients (n = 45). The cohort of patients who underwent sensory assessment had no cervical or lumbar spondylosis, carpal tunnel syndrome, type I diabetes or pharmacotherapy associated with sensory symptoms. Methods for genetic screening for hexanucleotide repeat expansions in *C9orf72* have been described previously [70]. Repeat-primed PCR was used and expansions longer than 30 repeats were considered pathological.

### *2.2 Sensory assessment*

Forty-five patients with ALS were systematically assessed for clinical signs of sensory dysfunction. Nociception was assessed using a 'neurotip' on the face, upper limbs and lower limbs bilaterally. Vibrioception and proprioception were assessed in the upper and lower limbs bilaterally. For nociception, vibrioception and proprioception, a score of '2' indicated normal sensation in the relevant body region, '1' indicated reduced sensation, and '0' indicated sensory loss in the investigated sensory domain. Graphaestesia, the ability to recognise symbols traced on the skin, and stereognosis, the ability to perceive the form of solid objects by touch, were assessed in the upper limbs bilaterally. For graphaestesia and stereognosis, the patient was given a score of '1' for each correct answer, and '0' for each incorrect answer. A composite score of 84 indicated no sensory deficits and lower scores corresponded with more severe sensory deficits.

### *2.3 Screening for sensory symptoms*

Additionally, a brief 7-item questionnaire was administered to screen for subjective symptoms pertaining to (1) upper limb paraesthesia, (2) lower limb paraesthesia, (3) cold sensitivity, (4) perioral paraesthesia, (5) tongue numbness, (6) changes in taste and (7) deterioration in sense of smell. Each item was scored 0–2, '0' meaning no symptoms in the relevant sensory domain.

### *2.4 Magnetic resonance imaging*

Images were acquired on a 3 Tesla Philips Achieva Magnetic resonance (MR) platform as part of a standardised neuroimaging protocol. T1-weighted (T1w) images were acquired with a 3D Inversion Recovery prepared Spoiled Gradient Recalled echo (IR-SPGR) sequence with the following key parameters: field-of-view (FOV) of 256 × 256 × 160 mm, flip angle = 8°, spatial resolution of 1 $mm^3$, SENSE factor = 1.5, TR/TE = 8.5/3.9 ms, TI = 1060 ms. Diffusion tensor images (DTI) data were acquired with a spin-echo echo planar imaging (SE-EPI) pulse sequence with a 32-direction Stejskal-Tanner diffusion encoding scheme; FOV = 245 × 245 × 150 mm, 60 slices with no interslice gap, spatial resolution = 2.5 $mm^3$, TR/TE = 7639/59 ms, SENSE factor = 2.5, b-values = 0, 1100 $s/mm^2$, dynamic stabilisation and spectral presaturation with inversion recovery (SPIR) fat suppression. Fluid-attenuated inversion recovery (FLAIR) images were acquired with an Inversion Recovery Turbo Spin Echo (IR-TSE) sequence to screen for comorbid inflammatory or vascular pathologies.

**Table 1. Panel of anatomical regions evaluated; key functions and connections.**

| Anatomical regions | Main functions | Key connections |
|---|---|---|
| Cortical regions | | |
| Postcentral gyrus | -primary somatosensory cortex<br>-processing afferent somatosensory inputs (touch, pressure, pain and temperature)<br>-integration of sensory and motor inputs necessary for skilled movement | -third-order neurons from thalamic VPL and VM ascend to the primary somatosensory cortex<br>-visual and auditory cortices<br>-subcortical structures encoding sensory modalities<br>-motor cortex |
| Insula | -multimodal sensory integration, interoception, perceptual self-awareness, autonomic control and emotional guidance of social behaviour<br><br>-posterior insula receives inputs from pain, temperature, visceral, and vestibular pathways, which are processed in mid-insular cortex and transferred to anterior insula for further processing and interaction with areas involved in cognitive and emotional control | Posterior insula:<br>-projects to lateral and central amygdaloid nuclei<br>-connects reciprocally with the secondary somatosensory cortex<br>-receives input from ventral posterior inferior and VM nuclei of thalamus<br>Anterior insula:<br>-projects to anterior amygdaloid area (AAA) and lateral, medial, cortical, accessory basal magnocellular and medial basal amygdaloid nuclei |
| Supramarginal gyrus | -part of the somatosensory association cortex<br>-interprets tactile sensory data and involved in perception of space and limb location<br>-involved in identifying postures and gestures of other people, a part of the mirror neuron system | -located just anterior to the angular gyrus<br>-these two structures make up the inferior parietal lobule forming a multimodal complex that interprets somatosensory, visual, and auditory information |
| Lateral occipital cortex | -object recognition and visual object processing<br>-facial recognition and motion perception | -middle longitudinal fasciculus, inferior longitudinal fasciculus, vertical occipital fasciculus, inferior fronto-occipital fasciculus, optic radiations, and U-shaped fibres connect lateral occipital lobe to itself as well as parts of the temporal, parietal, and medial occipital cortices |
| Superior temporal gyrus | -location of part of primary auditory cortex<br>-part of the high-order associative auditory cortex<br>-encodes sound features that are more complex and heterogeneous<br>-contains Wernicke's area (dominant cerebral hemisphere) | -auditory radiation from medial geniculate body to primary auditory cortex |
| Transverse temporal gyrus | -Also known as Heschl's gyrus<br>-Location of primary auditory cortex | -auditory radiation from medial geniculate body to primary auditory cortex |
| Thalamic nuclei | | |
| Ventral posterolateral | somatic sensation for contralateral trunk and limbs | -somatic afferents from trunk and limbs<br>-efferents to somatic sensory cortex |
| Ventromedial | somatic sensation for contralateral head/face | -somatic afferents from head<br>-efferents to somatic sensory cortex |
| Lateral posterior | -determining visual saliency, visually guided behaviours and multisensory processing of information related to aversive stimuli | -afferents from superior colliculus, primary visual, auditory and somatosensory cortex<br>-efferents to parietal association cortex |

**Table 1. Continued.**

| Anatomical regions | Main functions | Key connections |
|---|---|---|
| Lateral geniculate | -primary visual relay centre that receives retinofugal fibers and transmits visual information to the visual cortex | -afferent from optic tract<br>-efferent to primary visual cortex |
| Medial geniculate | -central role in auditory processing | -afferent from brachium of inferior colliculus<br>-efferent to primary auditory cortex |
| Amygdalar nuclei | | |
| Lateral nucleus | -involved in tactile, auditory, visual, olfactory, nociceptive processes as well as cognition and attention | -subcortical afferents–VP nucleus of thalamus, MGN, hypothalamus, midbrain reticular formation, cerulean nucleus<br>-cortical afferents–parietal, superior temporal gyrus, occipital, piriform lobe, hippocampus/entorhinal cortex, insula, orbital cortex, Basal nucleus of Meynert<br>-receives extrinsic sensory inputs and sends projections to other amygdala nuclei |
| Medial nucleus | -generates innate emotional responses to chemosignals<br>-key role in innate emotional behaviours, relaying olfactory information to hypothalamic nuclei involved in reproduction and defence | -termination of olfactory fibres from olfactory bulb<br>-projections to ventromedial nucleus of hypothalamus |
| Cortical nucleus | -processing of pheromonal information and olfaction<br>-presumably participates in ingestive, defensive and reproductive behaviours as a part of the vomeronasal amygdala | -termination of olfactory fibres from olfactory bulb<br>-projections to ventromedial nucleus of hypothalamus |
| White matter | | |
| Medial lemniscus | -part of the dorsal column-medial lemniscus pathway<br>-transmits proprioception, touch and vibration | -internal arcuate fibres cross over at great sensory decussation then ascend as the medial lemniscus, synapsing at VPL nucleus of thalamus |
| Posterior thalamic radiation | -connect the caudal parts of the thalamus with the parietal and occipital lobes through posterior thalamic peduncle and posterior limb of the internal capsule | -connect thalamus, parietal and occipital lobes |

AAA, anterior amygdaloid area; MGN, Medial geniculate nucleus; VM, Ventromedial nucleus; VP, ventral posterior nucleus; VPL, Ventral posterolateral nucleus.

**Table 2. The demographic and clinical profile of study participants.**

| Study groups | C9+ ALS | C9- ALS | HC | *p* value |
|---|---|---|---|---|
| | n = 22 | n = 138 | n = 127 | |
| Age (years) | 59.05 (6.176) | 61.46 (10.161) | 59.30 (10.960) | 0.195 |
| Sex (male) | 13 (59.09%) | 81 (58.70%) | 74 (58.27%) | 0.996 |
| Onset (bulbar) | 2 (9.09%) | 22 (15.94%) | N/a | 0.403 |
| Onset (spinal) | 20 (90.91%) | 116 (84.06%) | N/a | 0.403 |
| Handedness (right) | 19 (86.36%) | 122 (88.41%) | 112 (88.19%) | 0.963 |
| ALSFRS-R | 37.91 (6.852) | 37.17 (6.121) | N/a | 0.604 |

ALSFRS-r, revised ALS functional rating scale.

FLAIR data were acquired in axial orientation: FOV = 230 × 183 × 150 mm, spatial resolution = 0.65 × 0.87 × 4 mm, 30 slices with 1 mm gap, TR/TE = 11,000/125 ms, TI = 2800 ms, 120° refocusing pulse, with flow compensation and motion smoothing and a saturation slab covering the neck region. Clinical sequences (T1w and FLAIR) were radiologically reviewed for incidental findings and datasets from all participants underwent quality control review for movement artifacts before computational analyses.

### *2.5 Grey matter metrics*

The standard anatomical reconstruction pipeline of the FreeSurfer image analysis suite [71], was implemented, including non-parametric non-uniform intensity normalization, affine registration to the MNI305 atlas, intensity normalization, skull striping, automatic subcortical segmentation, linear volumetric registration, neck removal, tessellation of the grey matter-white matter boundary, surface smoothing, inflation to minimize metric distortion, and automated topology correction [72]. The relevant cortical labels of the Desikan-Killiany atlas were utilized to retrieve average cortical thickness and cortical volumes values from the postcentral gyrus, insula, superior temporal, transverse temporal, supramarginal, and lateral occipital cortices in the left and right cerebral hemispheres separately. The thalamus was parcellated into 25 sub-regions by Bayesian inference using a probabilistic atlas developed based on histological data [73]. The volumes of the following thalamic nuclei were evaluated in the two hemispheres separately: ventral posterolateral (VPL), ventromedial (VM), lateral posterior (LP), lateral geniculate (LGN), medial geniculate (MGN). The amygdala was segmented into 9 sub-regions using a probabilistic atlas developed based on histological [73,74]. The volumes of the lateral (LN), medial (MN), and cortical nuclei (CN) were estimated in each hemispheres separately.

### *2.6 White matter metrics*

Raw diffusion tensor data were eddy current corrected, skull stripped, and a tensor model was fitted in FMRIB's software library to create maps of axial diffusivity (AD), fractional anisotropy (FA), mean diffusivity (MD), and radial diffusivity (RD). FSL's tract-based statistics (TBSS) module was implemented for non-linear registration, skeletonisation and the creation of a mean FA mask. Diffusivity values were retrieved from the four (AD, FA, MD, RD) concatenated diffusivity files using the medial lemniscus and posterior thalamic radiation labels of the ICBM-DTI-81 white-matter atlas [75].

### *2.7 Statistics*

Assumptions of normality were examined using the Kolmogorov-Smirnov test. Skewness and kurtosis were assessed separately for each study group. Since all variables followed a normal distribution, parametric statistics were applied. The age and ALSFRS-r profile of the study groups were compared multivariate analysis of variance (MANOVA). Sex, symptom onset and handedness proportions in the study groups were contrasted using Pearson's chi-squared test. White matter variables and cortical thickness measures were contrasted using multivariate analysis of covariance (MANCOVA) with age and sex and covariates. Volumetric profiles (cortical, thalamic nuclei, amygdalar nuclei) of the study groups were also appraised in MANCOVAs with the following covariates, age, sex and total intracranial volume (TIV). Bonferroni corrections were used to account for multiple comparisons and reduce Type I error. Output statistics were summarised in comprehensive tables to report estimated marginal means (EMM), standard error (SE), *p*-values and post hoc pairwise comparisons. To further illustrate focal pathology, radar plots were generated for the two patients groups where EMMs were expressed as the percentage of reference (HC) EMM in the given anatomical region.

## 3. Results

### *3.1 Demographic profiles*

The study groups were matched for age, sex and handedness. Patient groups were matched for site of onset and functional disability (Table 2). Forty-five patients were specifically evaluated for the presence of sensory signs and symptoms, and all of these patients tested negative for the *C9orf72* gene.

**Table 3. Clinical sensory assessment scores in *C9orf72* negative patients (n = 45) [A] Lower scores indicate more severe sensory deficits on examination. [B] With regards to symptoms, lower scores indicate milder manifestations, '0' denotes no symptom in the relevant sensory domain.**

| | Scores | % of patients with some deficit | Min. Score | Max. Score | Mean | Std. Deviation |
|---|---|---|---|---|---|---|
| Sensory deficits[A] | Nociception (0–36) | 57.8 | 21 | 36 | 33.47 | 3.641 |
| | Vibrioception (0–24) | 80.0 | 6 | 24 | 19.16 | 4.537 |
| | Proprioception (0–12) | 28.9 | 6 | 12 | 11.49 | 1.141 |
| | Graphaesthesia (0–6) | 48.9 | 2 | 6 | 4.98 | 1.234 |
| | Stereognosis (0–6) | 28.9 | 2 | 6 | 5.51 | 0.944 |
| | Total deficit score (0–84) | 95.6 | 48 | 84 | 74.60 | 7.381 |
| Symptoms[B] | Paraesthesia hands/fingers (0–2) | 33.3 | 0 | 2 | 0.42 | 0.656 |
| | Paraesthesia feel/toes (0–2) | 20.0 | 0 | 2 | 0.29 | 0.626 |
| | Cold sensitivity hands/fingers (0–2) | 24.4 | 0 | 2 | 0.38 | 0.716 |
| | Tingling around lips (0–2) | 8.9 | 0 | 2 | 0.11 | 0.383 |
| | Tongue numbness (0–2) | 11.1 | 0 | 2 | 0.16 | 0.475 |
| | Changes in taste (0–2) | 24.4 | 0 | 2 | 0.33 | 0.640 |
| | Changes in smell (0–2) | 17.8 | 0 | 2 | 0.22 | 0.517 |
| | Total Symptoms Score (0–14) | 68.9 | 0 | 6 | 1.89 | 1.921 |

Number of patients systematically assessed n = 45, CN-V, Trigeminal nerve; LLL, left lower limb; LUL, left upper limb; RLL, right lower limb; RUL, right upper limb.

### *3.2 Clinical signs and symptoms*

On clinical examination, vibrioception was the most commonly affected sensory domain detected in 80.0% of the patients, subtle nociceptive deficits were identified in 57.8%, and proprioceptive deficits were ascertained in 28.9% of patients. Graphaesthesia was abnormal in 48.9% and stereognosis was abnormal in 28.9% of the 45 patients who had a dedicated sensory assessment at the time of their scan. Subtle facial sensory deficits were identified in 11.1% of patients. On the sensory symptom questionnaire, 68.9% reported at least one sensory symptom, and only 31.1% patients reported having no sensory symptoms at all. 33.3% had paraesthesia in the hands/fingers, 20% had paraesthesia in the feet/toes and 24.4% of patients reported cold sensitivity in hands/fingers. Tingling around the lips was reported in 8.9% and tongue numbness in 11.1%. 24.4% reported changes in taste and 17.8% of patients reported some change in smell (Table 3).

### *3.3 Cortical alterations*

C9- ALS patients exhibited cortical volume reductions in the insula bilaterally, and the left supramarginal and right superior temporal gyrus compared to healthy controls (Table 4). Each cortical region associated with sensory processing showed atrophic change in C9+ ALS bilaterally in comparison to both healthy controls and to C9- ALS. C9- ALS patients showed cortical thickness reductions in all evaluated regions except the lateral occipital region bilaterally and the right postcentral cortex. Cortical thickness changes were observed in all regions bilaterally in C9+ ALS in contrast to healthy controls, and in all regions except the transverse temporal bilaterally and the right insula when compared to C9- ALS (Fig. 1).

### *3.4 Subcortical nuclear degeneration*

In C9- ALS, volumes of all thalamic nuclei involved in sensory processing were reduced except the lateral geniculate nucleus (LGN) bilaterally and the left lateral posterior nucleus (Table 5). Sensory nuclei volumes were also reduced in C9+ ALS in comparison to healthy controls bilaterally except in the left medial geniculate nucleus. In the amygdalae of C9- ALS patients, volumetric reduction was observed in the right lateral and right cortical nuclei in comparison to healthy controls. Volumes reductions were also observed in the amygdalae of C9+ ALS patients in comparison to healthy controls in the lateral and cortical nuclei bilaterally and the left medial nucleus. When C9+ ALS patients are contrasted with C9- ALS patients, the volume of the left lateral nucleus was observed to be significantly reduced.

### *3.5 White matter alterations*

Significant inter-group AD and MD differences were observed in the right medial lemniscus and post hoc comparisons revealed AD differences between C9+ ALS and C9- ALS patients ($p = 0.038$). A trend of FA reduction was observed in C9- ALS compared to healthy controls in the left medial lemniscus ($p = 0.054$) (Table 6). FA reductions and increased RD were observed in the bilateral posterior thalamic radiation in both C9+ and C9- ALS in comparison to healthy controls. Increased posterior thalamic radiation MD was also detected in C9- ALS in contrast to healthy controls in the right hemisphere (Fig. 2).

**Table 4. Cortical grey matter volumes ($mm^3$) and cortical thickness (mm) in *C9orf72* positive ALS patients (C9+ ALS), *C9orf72* negative ALS patients (C9- ALS) and healthy controls (HC). For cortical volume values, estimated marginal means and standard error are adjusted for age (60.32), sex (1.41) and total intracranial volume (TIV) (1542959.99). For cortical thickness values, estimated marginal means and standard error are adjusted for age (60.32) and sex (1.41).**

| | Structure | Study group | EMM | Standard error | *p* value | Post-hoc comparisons | | |
|---|---|---|---|---|---|---|---|---|
| | | | | | | C9+ vs HC | C9- vs HC | C9+ vs C9- |
| Cortical Volumes | left postcentral | C9+ ALS | 7916.754 | 239.708 | **<0.001** | **<0.001** | 0.862 | **<0.001** |
| | | C9- ALS | 8983.901 | 96.087 | | | | |
| | | HC | 9132.497 | 99.762 | | | | |
| | right postcentral | C9+ ALS | 7610.712 | 227.482 | **<0.001** | **<0.001** | 1.000 | **<0.001** |
| | | C9- ALS | 8711.645 | 91.186 | | | | |
| | | HC | 8757.073 | 94.673 | | | | |
| | left insula | C9+ ALS | 6309.209 | 162.726 | **<0.001** | **<0.001** | **0.037** | **0.005** |
| | | C9- ALS | 6873.812 | 65.229 | | | | |
| | | HC | 7111.916 | 67.723 | | | | |
| | right insula | C9+ ALS | 6234.165 | 169.753 | **<0.001** | **<0.001** | **0.032** | **0.003** |
| | | C9- ALS | 6853.342 | 68.045 | | | | |
| | | HC | 7107.363 | 70.648 | | | | |
| | left supramarginal | C9+ ALS | 9121.066 | 301.457 | **<0.001** | **<0.001** | **0.024** | **<0.001** |
| | | C9- ALS | 10569.938 | 120.839 | | | | |
| | | HC | 11039.497 | 125.460 | | | | |
| | right supramarginal | C9+ ALS | 8268.990 | 278.070 | **<0.001** | **<0.001** | 0.258 | **<0.001** |
| | | C9- ALS | 9426.911 | 111.464 | | | | |
| | | HC | 9705.642 | 115.727 | | | | |
| | left lateral occipital | C9+ ALS | 10573.185 | 317.292 | **0.002** | **0.014** | 0.490 | **0.001** |
| | | C9- ALS | 11804.076 | 127.186 | | | | |
| | | HC | 11546.145 | 132.051 | | | | |
| | right lateral occipital | C9+ ALS | 10313.655 | 315.875 | **<0.001** | **<0.001** | 1.000 | **<0.001** |
| | | C9- ALS | 11854.095 | 126.618 | | | | |
| | | HC | 11726.933 | 131.461 | | | | |
| | left superior temporal | C9+ ALS | 10641.573 | 318.005 | **<0.001** | **<0.001** | 0.073 | **0.003** |
| | | C9- ALS | 11774.368 | 127.472 | | | | |
| | | HC | 12193.572 | 132.347 | | | | |
| | right superior temporal | C9+ ALS | 9812.695 | 269.843 | **<0.001** | **<0.001** | **<0.001** | **0.001** |
| | | C9- ALS | 10910.344 | 108.167 | | | | |
| | | HC | 11530.403 | 112.303 | | | | |
| | left transverse temporal | C9+ ALS | 1006.992 | 44.887 | **0.003** | **0.002** | 0.361 | **0.033** |
| | | C9- ALS | 1131.138 | 17.993 | | | | |
| | | HC | 1171.835 | 18.681 | | | | |
| | right transverse temporal | C9+ ALS | 776.246 | 33.451 | **0.001** | **0.001** | 0.653 | **0.010** |
| | | C9- ALS | 883.787 | 13.409 | | | | |
| | | HC | 907.819 | 13.922 | | | | |

**Table 4. Continued.**

| | Structure | Study group | EMM | Standard error | *p* value | Post-hoc comparisons | | |
|---|---|---|---|---|---|---|---|---|
| | | | | | | C9+ vs HC | C9- vs HC | C9+ vs C9- |
| Cortical Thickness | left postcentral | C9+ ALS | 1.857 | 0.025 | **<0.001** | **<0.001** | **0.012** | **<0.001** |
| | | C9- ALS | 1.998 | 0.010 | | | | |
| | | HC | 2.041 | 0.011 | | | | |
| | right postcentral | C9+ ALS | 1.859 | 0.025 | **<0.001** | **<0.001** | 0.080 | **<0.001** |
| | | C9- ALS | 1.986 | 0.010 | | | | |
| | | HC | 2.018 | 0.010 | | | | |
| | left insula | C9+ ALS | 2.691 | 0.039 | **<0.001** | **<0.001** | **0.001** | **<0.001** |
| | | C9- ALS | 2.855 | 0.015 | | | | |
| | | HC | 2.940 | 0.016 | | | | |
| | right insula | C9+ ALS | 2.765 | 0.039 | **<0.001** | **<0.001** | **<0.001** | 0.053$^{t}$ |
| | | C9- ALS | 2.864 | 0.015 | | | | |
| | | HC | 2.961 | 0.016 | | | | |
| | left supramarginal | C9+ ALS | 2.270 | 0.029 | **<0.001** | **<0.001** | **<0.001** | **<0.001** |
| | | C9- ALS | 2.439 | 0.012 | | | | |
| | | HC | 2.508 | 0.012 | | | | |
| | right supramarginal | C9+ ALS | 2.249 | 0.028 | **<0.001** | **<0.001** | **<0.001** | **<0.001** |
| | | C9- ALS | 2.396 | 0.011 | | | | |
| | | HC | 2.473 | 0.012 | | | | |
| | left lateral occipital | C9+ ALS | 2.012 | 0.027 | **<0.001** | **<0.001** | 1.000 | **<0.001** |
| | | C9- ALS | 2.130 | 0.011 | | | | |
| | | HC | 2.130 | 0.011 | | | | |
| | right lateral occipital | C9+ ALS | 2.036 | 0.024 | **<0.001** | **<0.001** | 1.000 | **<0.001** |
| | | C9- ALS | 2.143 | 0.010 | | | | |
| | | HC | 2.144 | 0.010 | | | | |
| | left superior temporal | C9+ ALS | 2.551 | 0.036 | **<0.001** | **<0.001** | **<0.001** | **0.027** |
| | | C9- ALS | 2.652 | 0.014 | | | | |
| | | HC | 2.766 | 0.015 | | | | |
| | right superior temporal | C9+ ALS | 2.591 | 0.036 | **<0.001** | **<0.001** | **<0.001** | **0.026** |
| | | C9- ALS | 2.694 | 0.015 | | | | |
| | | HC | 2.832 | 0.015 | | | | |
| | left transverse temporal | C9+ ALS | 2.206 | 0.046 | **<0.001** | **0.002** | **0.010** | 0.178 |
| | | C9- ALS | 2.300 | 0.018 | | | | |
| | | HC | 2.378 | 0.019 | | | | |
| | right transverse temporal | C9+ ALS | 2.213 | 0.051 | **0.001** | **0.001** | **0.025** | 0.102 |
| | | C9- ALS | 2.330 | 0.020 | | | | |
| | | HC | 2.409 | 0.021 | | | | |

Significant intergroup differences at $p < 0.05$ after Bonferroni correction for multiple comparisons are highlighted in bold print, $^{t}$ indicates a statistical trend of $0.05 < p_{cor} < 0.07$.

## 4. Discussion

While ALS is primarily associated with motor and frontotemporal dysfunction [76–80], we have demonstrated the degeneration of anatomical structures involved in somatosensory, visual and auditory processing. Both cortical volumes and cortical thickness were significantly reduced in the postcentral, insular, supramarginal, lateral occipital, superior temporal and transverse temporal cortices bilaterally in C9+ ALS patients in comparison to healthy controls. Bilateral insular, supramarginal, superior temporal and transverse temporal as well as left postcentral cortical thickness reductions were also observed in C9- ALS patients.

**Table 5. Thalamic and amygdalar nuclear volumes ($mm^3$) in *C9orf72* positive ALS patients (C9+ ALS), *C9orf72* negative ALS patients (C9- ALS) and healthy controls (HC). Estimated Marginal Means And Standard Error Are Adjusted For Age (60.32), Sex (1.41) And Total Intracranial Volume (TIV) (1542959.99).**

| Structure | Study group | EMM | standard error | *p* value | Post-hoc comparisons | | |
|---|---|---|---|---|---|---|---|
| | | | | | C9+ vs HC | C9- vs HC | C9+ vs C9- |
| left thalamus proper | C9+ ALS | 6279.851 | 154.835 | **<0.001** | **<0.001** | **0.002** | **<0.001** |
| | C9- ALS | 6968.154 | 62.066 | | | | |
| | HC | 7282.553 | 64.439 | | | | |
| right thalamus proper | C9+ ALS | 5922.869 | 137.042 | **<0.001** | **<0.001** | **0.002** | **<0.001** |
| | C9- ALS | 6593.957 | 54.933 | | | | |
| | HC | 6873.343 | 57.034 | | | | |
| left ventral posterolateral (thalamus) | C9+ ALS | 808.611 | 23.181 | **<0.001** | **0.004** | **<0.001** | 1.000 |
| | C9- ALS | 821.560 | 9.292 | | | | |
| | HC | 890.153 | 9.647 | | | | |
| right ventral posterolateral (thalamus) | C9+ ALS | 740.267 | 20.922 | **<0.001** | **0.003** | **<0.001** | 0.617 |
| | C9- ALS | 768.988 | 8.386 | | | | |
| | HC | 815.432 | 8.707 | | | | |
| left ventromedial (thalamus) | C9+ ALS | 18.802 | 0.590 | **<0.001** | **0.001** | **<0.001** | 1.000 |
| | C9- ALS | 19.396 | 0.236 | | | | |
| | HC | 21.230 | 0.245 | | | | |
| right ventromedial (thalamus) | C9+ ALS | 17.468 | 0.638 | **<0.001** | **<0.001** | **<0.001** | 0.404 |
| | C9- ALS | 18.504 | 0.256 | | | | |
| | HC | 20.158 | 0.266 | | | | |
| left lateral posterior (thalamus) | C9+ ALS | 94.283 | 4.323 | **<0.001** | **<0.001** | $0.062^t$ | **0.002** |
| | C9- ALS | 110.495 | 1.733 | | | | |
| | HC | 116.344 | 1.799 | | | | |
| right lateral posterior (thalamus) | C9+ ALS | 88.676 | 3.816 | **<0.001** | **<0.001** | **0.017** | **0.004** |
| | C9- ALS | 102.224 | 1.530 | | | | |
| | HC | 108.403 | 1.588 | | | | |
| left lateral geniculate nucleus | C9+ ALS | 146.082 | 5.403 | **<0.001** | **<0.001** | 0.510 | **0.004** |
| | C9- ALS | 165.165 | 2.166 | | | | |
| | HC | 169.490 | 2.249 | | | | |
| right lateral geniculate nucleus | C9+ ALS | 139.186 | 5.126 | **0.001** | **<0.001** | 1.000 | **0.002** |
| | C9- ALS | 158.301 | 2.055 | | | | |
| | HC | 160.663 | 2.133 | | | | |
| left medial geniculate nucleus | C9+ ALS | 103.127 | 3.749 | **0.030** | 0.425 | **0.036** | 1.000 |
| | C9- ALS | 103.568 | 1.503 | | | | |
| | HC | 109.090 | 1.560 | | | | |
| right medial geniculate nucleus | C9+ ALS | 96.508 | 3.267 | **0.002** | **0.009** | **0.021** | 0.395 |
| | C9- ALS | 101.851 | 1.309 | | | | |
| | HC | 107.026 | 1.360 | | | | |
| left lateral nucleus (amygdala) | C9+ ALS | 587.603 | 18.059 | **<0.001** | **0.001** | 0.094 | **0.029** |
| | C9- ALS | 638.607 | 7.239 | | | | |
| | HC | 661.328 | 7.516 | | | | |
| right lateral nucleus (amygdala) | C9+ ALS | 621.303 | 17.962 | **<0.001** | **0.002** | **0.015** | 0.170 |
| | C9- ALS | 658.510 | 7.200 | | | | |
| | HC | 688.082 | 7.476 | | | | |

**Table 5. Continued.**

| Structure | Study group | EMM | standard error | *p* value | Post-hoc comparisons | | |
|---|---|---|---|---|---|---|---|
| | | | | | C9+ vs HC | C9- vs HC | C9+ vs C9- |
| left medial nucleus (amygdala) | C9+ ALS | 16.070 | 1.118 | **0.018** | **0.017** | 0.592 | 0.114 |
| | C9- ALS | 18.595 | 0.448 | | | | |
| | HC | 19.436 | 0.465 | | | | |
| right medial nucleus (amygdala) | C9+ ALS | 20.066 | 1.316 | 0.437 | 0.628 | 1.000 | 0.673 |
| | C9- ALS | 21.801 | 0.528 | | | | |
| | HC | 21.855 | 0.548 | | | | |
| left cortical nucleus (amygdala) | C9+ ALS | 20.734 | 1.055 | **0.001** | **0.001** | $0.050^{t}$ | 0.071 |
| | C9- ALS | 23.331 | 0.423 | | | | |
| | HC | 24.809 | 0.439 | | | | |
| right cortical nucleus (amygdala) | C9+ ALS | 23.693 | 0.978 | **<0.001** | **0.001** | **0.020** | 0.123 |
| | C9- ALS | 25.864 | 0.392 | | | | |
| | HC | 27.416 | 0.407 | | | | |

Significant intergroup differences at $p < 0.05$ after Bonferroni correction for multiple comparisons are highlighted in bold print, $^{t}$ indicates a statistical trend of $0.05 < p_{cor} < 0.07$.

The postcentral gyrus is the location of the primary somatosensory cortex which processes somatosensory inputs from the entire body and integrates sensory and motor signals. It is abundantly interconnected with subcortical structures encoding sensory modalities [81] and our data indicate that it is affected in both C9+ ALS and C9- ALS. Our data also confirm insular cortex degeneration irrespective of hexanucleotide repeat status. The insular cortex has ample connections to the secondary somatosensory cortex, sensory nuclei in the thalamus and the amygdala and is involved in multimodal sensory processing, interoception, autonomic control and integration of sensory signals with cognition and emotion. The supramarginal gyrus is part of the somatosensory association cortex and is involved in the perception of space and limb location and the interpretation of tactile sensory data. There is a benefit associated with evaluating multiple cortical measures as imaging indices have different sensitivity profiles to capture pathological changes. For example, left postcentral cortex involvement in C9- ALS was only detected on cortical thickness analyses. C9+ ALS patients predominantly exhibited symmetrical cortical changes, whereas C9- ALS patients showed more selective cortical pathology which was unilateral in certain regions.

We have confirmed previous reports of overall thalamus volume reduction in C9+ ALS [60], and additionally, demonstrated focal changes in nuclei relaying sensory information; the ventral posterolateral, ventromedial, lateral posterior and lateral geniculate nuclei bilaterally and right medial geniculate nucleus. In C9- ALS, we observed bilateral ventral posterolateral, ventromedial and medial geniculate nucleus degeneration as well as right lateral posterior nucleus pathology. Physiologically, the ventral posterolateral and ventromedial nuclei have a primary sensory function; they relay somatosensory information from the head and body. Our cross-sectional study captures the degeneration of structures involved in sensory processing both at a subcortical and cortical level. Longitudinal data are required to clarify the chronology of cortical and subcortical involvement which may then contribute to the corticofugal versus corticopetal spread debate [82–84].

The amygdala mediates a multitude of functions including reward processing, memory consolidation, fear conditioning etc., but also integrates somatosensory, visual, auditory, olfactory, gustatory and visceral sensory modalities. Amygdalar degeneration had been previously implicated in both ALS and in primary lateral sclerosis [85–88]. In our C9+ ALS cohort, volumes of the lateral and cortical nuclei bilaterally and the left medial nucleus were reduced. In C9- ALS patients, the volumes of the right lateral and cortical nuclei were reduced compared to healthy controls. The lateral nucleus is involved in relaying nociceptive, tactile, auditory, visual and olfactory processes. The medial nucleus is recipients of olfactory information and is also involved in pheromone-processing. The integration of our cortical and subcortical grey matter findings suggests that GGGGCC repeats in *C9orf72* are associated with more severe and more widespread degeneration of sensory regions compared to C9- ALS and these changes are more likely to be bilateral.

Overt visual symptoms are seldom experienced in ALS, but alterations in visual evoked potentials [47,48] and retinal changes on optical coherence tomography (OCT) [89] have been reported. Our radiological findings indicate that multiple components of the visual pathway are affected. Both the volume and thickness of the lateral occipital cortex which is involved in object and facial recognition, as well as the volume of the right lateral geniculate nucleus,

**Table 6. Axial diffusivity (AD), fractional Anisotropy (FA), mean diffusivity (MD) and radial diffusivity (RD) in *C9orf72* positive ALS patients (C9+ ALS), *C9orf72* negative ALS patients (C9- ALS) and healthy controls (HC). Estimated marginal means and standard error are adjusted for age (60.32) and sex (1.41).**

| Structure | Study group | EMM | standard error | $p$ value | Post-hoc comparisons | | |
|---|---|---|---|---|---|---|---|
| | | | | | C9+ vs HC | C9- vs HC | C9+ vs C9- |
| AD medial lemniscus left | C9+ ALS | 0.001148 | 0.000015 | 0.149 | 0.154 | 1.000 | 0.295 |
| | C9- ALS | 0.001174 | $5.853586 \times 10^{-6}$ | | | | |
| | HC | 0.001179 | $6.096982 \times 10^{-6}$ | | | | |
| AD medial lemniscus right | C9+ ALS | 0.001154 | $1.410245 \times 10^{-5}$ | **0.044** | 0.096 | 1.000 | **0.038** |
| | C9- ALS | 0.001192 | $5.644191 \times 10^{-6}$ | | | | |
| | HC | 0.001187 | $5.878880 \times 10^{-6}$ | | | | |
| FA medial lemniscus left | C9+ ALS | 0.568855 | 0.009018 | 0.212 | 1.000 | 0.322 | 0.805 |
| | C9- ALS | 0.558068 | 0.003609 | | | | |
| | HC | 0.566511 | 0.003759 | | | | |
| FA medial lemniscus right | C9+ ALS | 0.561060 | 0.008291 | $0.060^t$ | 1.000 | $0.054^t$ | 1.000 |
| | C9- ALS | 0.556778 | 0.003318 | | | | |
| | HC | 0.568222 | 0.003456 | | | | |
| MD medial lemniscus left | C9+ ALS | 0.000671 | $9.836082 \times 10^{-6}$ | 0.165 | 0.342 | 1.000 | 0.174 |
| | C9- ALS | 0.000691 | $3.936673 \times 10^{-6}$ | | | | |
| | HC | 0.000688 | $4.100363 \times 10^{-6}$ | | | | |
| MD medial lemniscus right | C9+ ALS | 0.000678 | $9.294528 \times 10^{-6}$ | **0.035** | 0.542 | 0.228 | $0.066^t$ |
| | C9- ALS | 0.000702 | $3.719929 \times 10^{-6}$ | | | | |
| | HC | 0.000692 | $3.874606 \times 10^{-6}$ | | | | |
| RD medial lemniscus left | C9+ ALS | 0.000433 | $9.959697 \times 10^{-6}$ | 0.188 | 1.000 | 0.605 | 0.331 |
| | C9- ALS | 0.000450 | $3.986148 \times 10^{-6}$ | | | | |
| | HC | 0.000443 | $4.151894 \times 10^{-6}$ | | | | |
| RD medial lemniscus right | C9+ ALS | 0.000441 | $9.336970 \times 10^{-6}$ | $0.058^t$ | 1.000 | 0.092 | 0.370 |
| | C9- ALS | 0.000456 | $3.736915 \times 10^{-6}$ | | | | |
| | HC | 0.000444 | $3.892298 \times 10^{-6}$ | | | | |
| AD posterior thalamic radiation left | C9+ ALS | 0.001265 | $1.389886 \times 10^{-5}$ | 0.312 | 0.387 | 1.000 | 0.667 |
| | C9- ALS | 0.001283 | $5.562710 \times 10^{-6}$ | | | | |
| | HC | 0.001288 | $5.794011 \times 10^{-6}$ | | | | |
| AD posterior thalamic radiation right | C9+ ALS | 0.001236 | $1.392658 \times 10^{-5}$ | 0.362 | 0.500 | 1.000 | 0.521 |
| | C9- ALS | 0.001256 | $5.573804 \times 10^{-6}$ | | | | |
| | HC | 0.001257 | $5.805567 \times 10^{-6}$ | | | | |
| FA posterior thalamic radiation left | C9+ ALS | 0.510931 | 0.008419 | **<0.001** | **<0.001** | **0.001** | 0.077 |
| | C9- ALS | 0.531271 | 0.003369 | | | | |
| | HC | 0.549686 | 0.003509 | | | | |
| FA posterior thalamic radiation right | C9+ ALS | 0.502567 | 0.008459 | **<0.001** | **<0.001** | **<0.001** | 0.078 |
| | C9- ALS | 0.522972 | 0.003385 | | | | |
| | HC | 0.542817 | 0.003526 | | | | |
| MD posterior thalamic radiation left | C9+ ALS | 0.000783 | $1.113229 \times 10^{-5}$ | 0.159 | 0.558 | 0.268 | 1.000 |
| | C9- ALS | 0.000778 | $4.455453 \times 10^{-6}$ | | | | |
| | HC | 0.000767 | $4.640713 \times 10^{-6}$ | | | | |
| MD posterior thalamic radiation right | C9+ ALS | 0.000770 | $1.040189 \times 10^{-5}$ | **0.035** | 0.363 | **0.046** | 1.000 |
| | C9- ALS | 0.000767 | $4.163127 \times 10^{-6}$ | | | | |
| | HC | 0.000752 | $4.336233 \times 10^{-6}$ | | | | |
| RD posterior thalamic radiation left | C9+ ALS | 0.000543 | $1.160346 \times 10^{-5}$ | **0.002** | **0.015** | **0.017** | 0.553 |
| | C9- ALS | 0.000526 | $4.644025 \times 10^{-6}$ | | | | |
| | HC | 0.000507 | $4.837127 \times 10^{-6}$ | | | | |
| RD posterior thalamic radiation right | C9+ ALS | 0.000537 | $1.088973 \times 10^{-5}$ | **<0.001** | **0.006** | **0.001** | 0.659 |
| | C9- ALS | 0.000522 | $4.358372 \times 10^{-6}$ | | | | |
| | HC | 0.000500 | $4.539596 \times 10^{-6}$ | | | | |

Significant intergroup differences at $p < 0.05$ after Bonferroni correction for multiple comparisons are flagged in bold print. $^t$ indicates a statistical trend of $0.05 < p_{cor} < 0.07$.

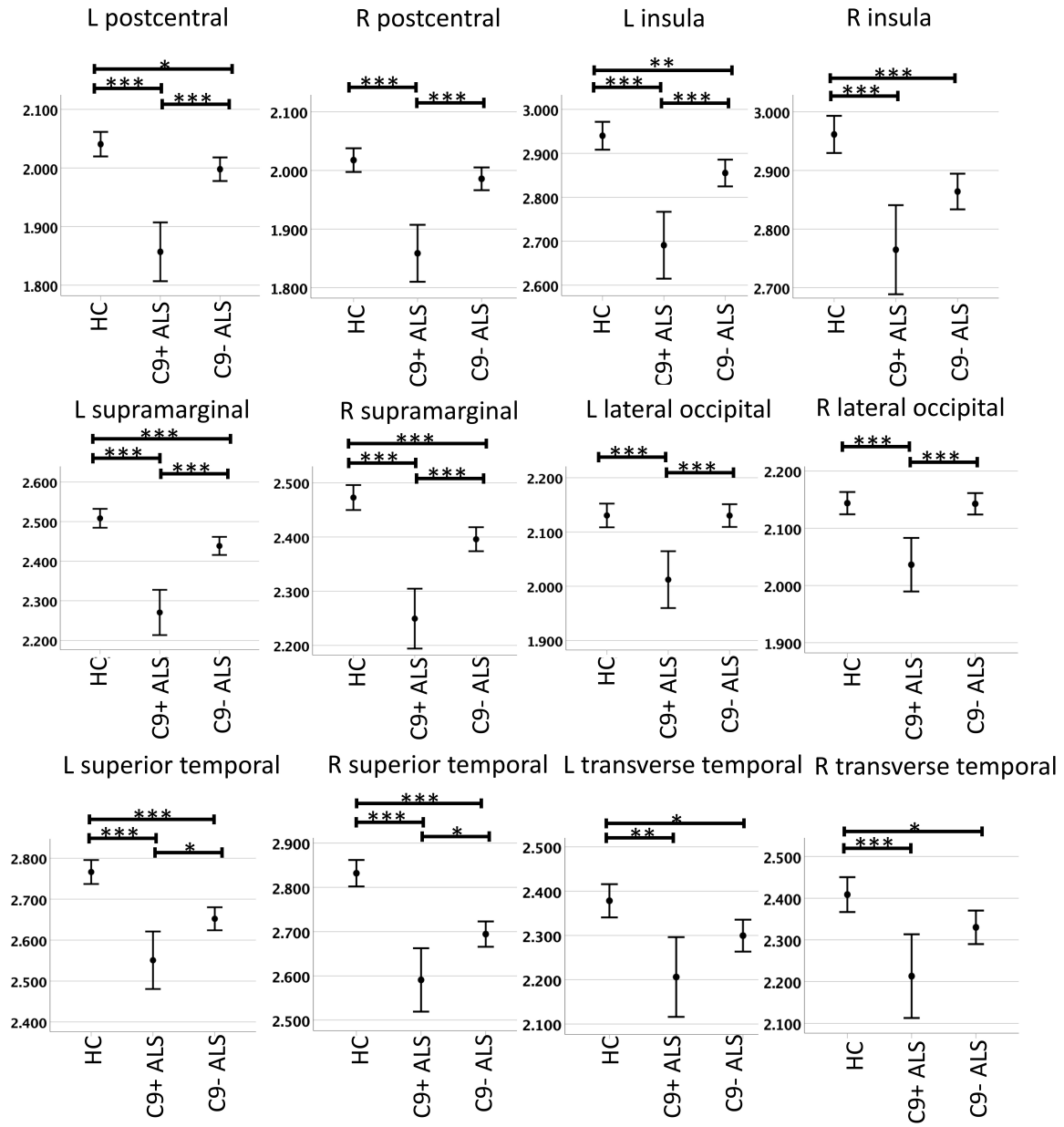


**Fig. 1. Cortical thickness profile in *C9orf72* positive ALS patients (C9+ ALS), *C9orf72* negative ALS patients (C9- ALS), healthy controls (HC), based on estimated marginal means adjusted for age and sex.** Error bars represent 95% confidence intervals. Left denoted by (L) and right denoted by (R). Significant inter-group differences corrected for multiple comparisons are highlighted with asterisks: * $p$ value between 0.01 and 0.05, ** $p$ value between 0.001 and 0.01, *** $p$ value $< 0.001$.

which is the primary visual relay centre to the visual cortex is reduced in C9+ ALS. Volume of the lateral posterior nucleus is reduced bilaterally in C9+ ALS, but only the right nucleus is reduced in C9- ALS. The lateral posterior nucleus has a role in visual saliency and visually guided behaviours with afferents from the superior colliculus, primary visual, auditory and somatosensory cortices and efferents to the parietal association cortex.

Hearing problems are not commonly associated with ALS, but abnormal auditory evoked potentials have also been reported [8,48]. Our imaging findings suggest the involvement of auditory pathways. In C9+ ALS, we detected cortical volume and thickness reductions in the superior temporal and transverse temporal cortices bilaterally and right medial geniculate nucleus atrophy. In C9- ALS, cortical thickness changes were noted in the superior temporal and transverse temporal cortices bilaterally and volume reductions in the right superior temporal cortex and medial geniculate nucleus bilaterally. The transverse temporal gyrus encompasses the primary auditory cortex and the superior temporal region includes the high-order associative auditory cortex and also possesses a number of non-

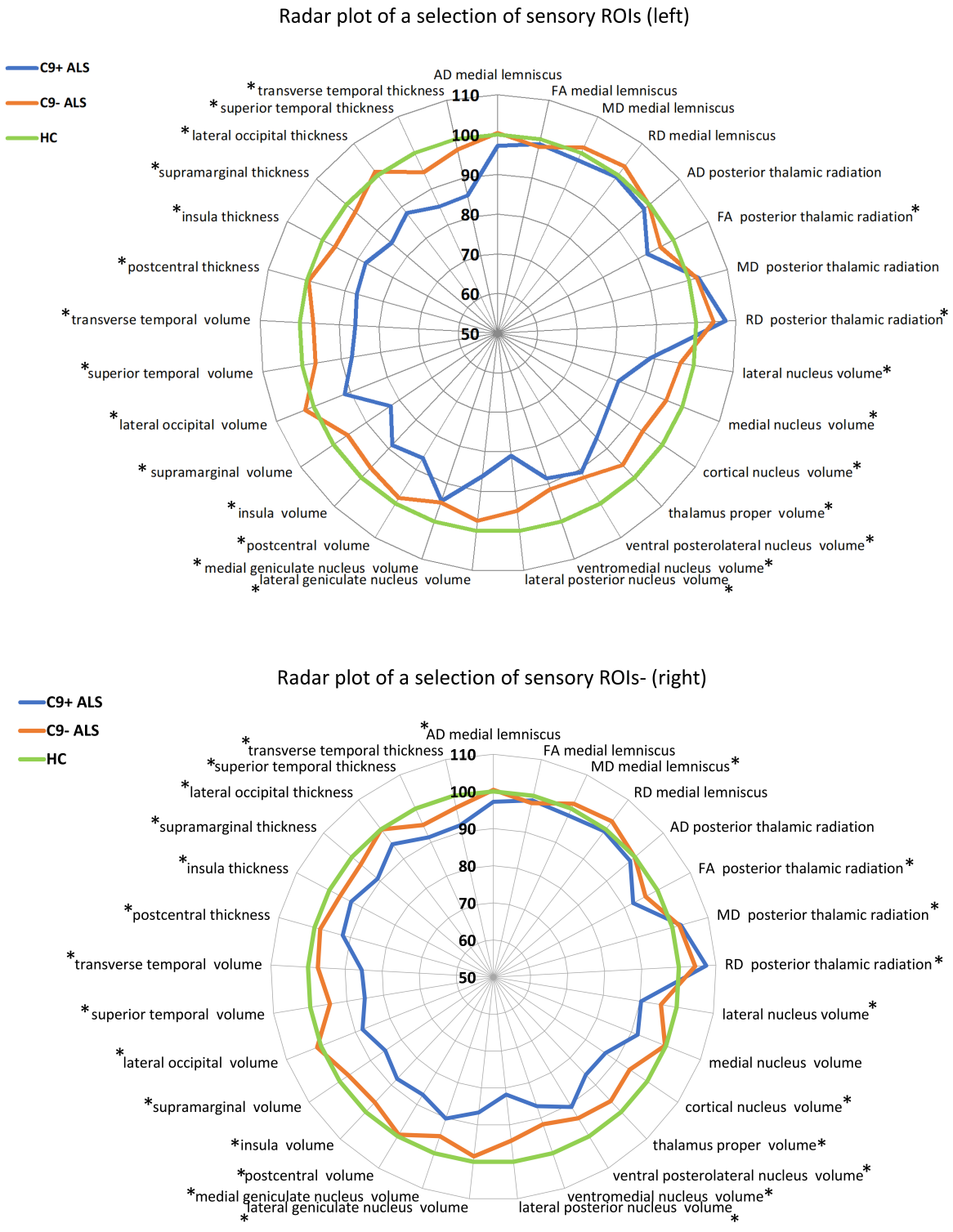


**Fig. 2. Radar plots of integrity measures expressed as % of estimated marginal means of controls (green) in regions of interest associated with sensory processing.** * indicates significant intergroup differences ($p$ value $< 0.05$).

sensory functions. The medial geniculate nucleus is a key hub of the auditory pathway and forms the thalamic relay between the inferior colliculus and the auditory cortex.

A key finding of this study is the demonstration of medial lemniscus involvement in ALS. Axial diffusivity differences have been captured between C9+ and C9- patients in the right medial lemniscus ($p = 0.038$) and there is a trend of reduced FA in the left medial lemniscus ($p = 0.054$) in C9- ALS compared to healthy controls. Despite the plethora of tractography studies in ALS [90,91], sensory white matter tracts are seldom evaluated specifically and brainstem studies typically focus on motor tract degen-

eration [92,93]. The medial lemniscus is part of the dorsal column-medial lemniscus pathway which transmits proprioception, touch and vibration. Internal arcuate fibres cross over at the great sensory decussation then ascend as the medial lemniscus, synapsing at the ventral posterolateral nucleus of the thalamus. The posterior thalamic radiation includes functionally diverse thalamocortical white matter projections encompassing sensory and non-sensory fibres which connect the caudal thalamus with the occipital and parietal lobes. FA reductions and increased RD were observed in the posterior thalamic radiation bilaterally in both C9+ and C9- ALS in comparison to healthy controls.

Complementary to established motor [79,94] and frontotemporal pathology [80,95], our results provide structural evidence of somatosensory pathway degeneration in both C9+ ALS and C9- ALS. We have detected evidence of multi-level pathological change spanning from the medial lemniscus, through the thalamic nuclei and thalamocortical radiation to the primary sensory cortex. Our data also provide evidence of the concomitant degeneration of cortical and subcortical components of the auditory and visual pathways. On clinical assessment, the majority of patients only exhibit limited sensory signs and report mild or no symptoms. Accordingly, the pathological changes observed on neuroimaging may be considered sub-clinical. While somatosensory, visual and auditory deficits are not routinely investigated, they may have significant implications for activities of daily living. Proprioceptive deficits may contribute to gait impairment, fall risk and impaired dexterity. The wider recognition of proprioceptive deficits may guide falls prevention strategies. Pharyngeal and laryngeal sensory deficits [39,40] may exacerbate dysphagia, and altered smell and impaired taste [35,36,96] may contribute to diminished appetite [37]. Changes in taste are likely to be multifactorial in ALS and may be exacerbated by other factors such as medications and oral candidiasis [35,36].

This study is not without limitations. We performed a cross-sectional imaging study of symptomatic ALS patients; the longitudinal interrogation of integrity metrics in these anatomical foci would provide important additional insights [82,97]. We purposefully did not explore direct clinico-radiological correlations between clinical scores and imaging findings, acknowledging the contribution of spinal [98] and peripheral components of the sensory system to clinical manifestations [69,98,99]. Our clinical data pertain to *C9orf72* negative patients only and we did not collect visual, auditory or olfactory clinical data to complement our neuroimaging findings. Some of the anatomical regions we assessed mediate exclusively sensory functions (postcentral gyrus, medial lemniscus etc.), but some of the regions we evaluated (posterior thalamic radiation, insula etc.) have both sensory and non-sensory roles and their degeneration is therefore less specific to sensory functions. While we have confirmed the involvement of cerebral hubs of sensory circuits, future studies of sensory dysfunction in ALS should acquire quantitative electrophysiology data to evaluate the spinal and peripheral components of sensory networks. Notwithstanding these limitations, we have demonstrated the degeneration of cortical, subcortical and white matter components of somatosensory pathways in a condition which is primarily associated with motor and frontotemporal dysfunction.

## 5. Conclusions

Key subcortical hubs, white matter tracts and cortical components of the somatosensory system are affected in ALS. ALS should no longer be regarded as a condition exclusively involving motor and frontotemporal regions. Subclinical or subtle sensory deficits may exacerbate mobility, impact on dexterity, increase fall risk and may have ramifications for bulbar dysfunction. Somatosensory deficits in ALS are important to recognise, should be routinely screened for, and should be taken into account when planning multidisciplinary interventions.

## Abbreviations

AAA, anterior amygdaloid area; AD, axial diffusivity; ALS, amyotrophic lateral sclerosis; ALSFRS-r, revised Amyotrophic Lateral Sclerosis Functional Rating Scale; C9- ALS, *C9orf72* negative ALS patients; C9+ ALS, *C9orf72* positive ALS patients; *C9orf72*, chromosome 9 open reading frame 72 gene; CHEP, contact heat-evoked potential; CN-V, Trigeminal nerve; CT, cortical thickness; DKI, diffusion kurtosis imaging; DTI, diffusion tensor imaging; EMM, estimated marginal mean; EPI, echo-planar imaging; FA, fractional anisotropy; FDA, United States Federal Drug Administration; FEEST, fibre-optic endoscopic evaluation of swallowing with sensory testing; FLAIR, fluid-attenuated inversion recovery; FOV, field of view; FTD, frontotemporal dementia; FWE, familywise error; GM, grey matter; HARDI, high angular resolution diffusion imaging; HC, healthy control; IR-SPGR, inversion recovery prepared spoiled gradient recalled echo; IR-TSE, inversion recovery turbo spin echo sequence; LGN, Lateral geniculate nucleus; LLL, left lower limb; LMN, lower motor neuron; Lt, Left; LUL, left upper limb; MD, mean diffusivity; MGN, Medial geniculate nucleus; MLe, Medial Lemniscus; MND, Motor neuron disease; MNI152, Montreal Neurological Institute 152 standard space; MRI, magnetic resonance imaging; NODDI, neurite orientation dispersion and density imaging; OCT, optical coherence tomography; PMC, primary motor cortex; PTR, Posterior Thalamic Radiation; QC, quality control; RD, radial diffusivity; RLL, right lower limb; RNFL, retinal nerve fibre layer; ROI, region of interest; Rt, right; RUL, right upper limb; SAPA, sensory action potential amplitude; SD, standard deviation; SE-EPI, spin-echo echo planar imaging; SENSE, sensitivity Encoding; SEP, somatosensory evoked potential; SNAP, sensory nerve action potential; *SOD1*, superoxide dismutase 1; SPIR, spectral presatura-

tion with inversion recovery; SWI, susceptibility weighted imaging; T1w, T1-weighted imaging; TBSS, tract-based spatial Statistics; TDP-43, TAR DNA-binding protein; TE, echo time; TFCE, threshold-free cluster enhancement; TI, inversion time; TIV, total intracranial volume; TR, repetition time; UMN, upper motor neuron; VEP, visual evoked potentials; VM, Ventromedial nucleus; VP ventral posterior nucleus; VPL, Ventral posterolateral nucleus; WM, white matter.

## Author contributions

Conceptualisation of the study—RHC, PB. Drafting the manuscript—RHC, GM, PB. Data collection—RHC, GM, PB. Neuroimaging analyses—RHC, AM, JL, PB. Revision of the manuscript for intellectual content—RHC, GM, AM, JL, OH, PB.

## Ethics approval and consent to participate

The study was approved by the Ethics Committee of Beaumont Hospital, Dublin, Ireland (REC ID: 08/90) and all participants provided written informed consent prior to inclusion.


## Acknowledgment

We express our gratitude to all patients and healthy controls for participating in this research study. Without their contribution, this study would not have been possible.

## Funding

PB and the Computational Neuroimaging Group are supported by the Health Research Board (HRB EIA-2017-019 and HRB JPND-Cofund2-2019-1), the Irish Institute of Clinical Neuroscience (IICN), the Spastic Paraplegia Foundation (SPF), the EU Joint Programme – Neurodegenerative Disease Research (JPND), the Andrew Lydon scholarship, and the Iris O'Brien Foundation.


## Conflict of interest

The authors declare no conflict of interest.

## References


[1] Sábado J, Casanovas A, Tarabal O, Hereu M, Piedrafita L, Calderó J, *et al*. Accumulation of misfolded SOD1 in dorsal root ganglion degenerating proprioceptive sensory neurons of transgenic mice with amyotrophic lateral sclerosis. BioMed Research International. 2014; 2014: 852163.

[2] Tao Q, Wei Q, Wu Z. Sensory nerve disturbance in amyotrophic lateral sclerosis. Life Sciences. 2018; 203: 242–245.

[3] Christidi F, Karavasilis E, Rentzos M, Kelekis N, Evdokimidis I, Bede P. Clinical and Radiological Markers of Extra-Motor Deficits in Amyotrophic Lateral Sclerosis. Frontiers in Neurology. 2018; 9: 1005.

[4] Hammad M, Silva A, Glass J, Sladky JT, Benatar M. Clinical, electrophysiologic, and pathologic evidence for sensory abnormalities in ALS. Neurology. 2007; 69: 2236–2242.

[5] Gubbay SS, Kahana E, Zilber N, Cooper G, Pintov S, Leibowitz Y. Amyotrophic lateral sclerosis. a study of its presentation and prognosis. Journal of Neurology. 1985; 232: 295–300.

[6] Isaacs JD, Dean AF, Shaw CE, Al-Chalabi A, Mills KR, Leigh PN. Amyotrophic lateral sclerosis with sensory neuropathy: part of a multisystem disorder? Journal of Neurology, Neurosurgery, and Psychiatry. 2007; 78: 750–753.

[7] Gregory R, Mills K, Donaghy M. Progressive sensory nerve dysfunction in amyotrophic lateral sclerosis: a prospective clinical and neurophysiological study. Journal of Neurology. 1993; 240: 309–314.

[8] Radtke RA, Erwin A, Erwin CW. Abnormal sensory evoked potentials in amyotrophic lateral sclerosis. Neurology. 1986; 36: 796–801.

[9] Iglesias C, Sangari S, El Mendili M, Benali H, Marchand-Pauvert V, Pradat P. Electrophysiological and spinal imaging evidences for sensory dysfunction in amyotrophic lateral sclerosis. BMJ Open. 2015; 5: e007659.

[10] Pugdahl K, Fuglsang-Frederiksen A, de Carvalho M, Johnsen B, Fawcett PRW, Labarre-Vila A, *et al*. Generalised sensory system abnormalities in amyotrophic lateral sclerosis: a European multicentre study. Journal of Neurology, Neurosurgery, and Psychiatry. 2007; 78: 746–749.

[11] Pugdahl K, Fuglsang-Frederiksen A, Johnsen B, de Carvalho M, Fawcett PRW, Labarre-Vila A, *et al*. A prospective multicentre study on sural nerve action potentials in ALS. Clinical Neurophysiology. 2008; 119: 1106–1110.

[12] Zhou C, Hu X, Hu J, Liang M, Yin X, Chen L, *et al*. Altered Brain Network in Amyotrophic Lateral Sclerosis: a Resting Graph Theory-Based Network Study at Voxel-Wise Level. Frontiers in Neuroscience. 2016; 10: 204.

[13] Devine MS, Pannek K, Coulthard A, McCombe PA, Rose SE, Henderson RD. Exposing asymmetric gray matter vulnerability in amyotrophic lateral sclerosis. NeuroImage. Clinical. 2015; 7: 782–787.

[14] Dalla Bella E, Lombardi R, Porretta-Serapiglia C, Ciano C, Gellera C, Pensato V, *et al*. Amyotrophic lateral sclerosis causes small fiber pathology. European Journal of Neurology. 2016; 23: 416–420.

[15] Isak B, Pugdahl K, Karlsson P, Tankisi H, Finnerup NB, Furtula J, *et al*. Quantitative sensory testing and structural assessment of sensory nerve fibres in amyotrophic lateral sclerosis. Journal of the Neurological Sciences. 2017; 373: 329–334.

[16] Nolano M, Provitera V, Manganelli F, Iodice R, Caporaso G, Stancanelli A, *et al*. Non-motor involvement in amyotrophic lateral sclerosis: new insight from nerve and vessel analysis in skin biopsy. Neuropathology and Applied Neurobiology. 2017; 43: 119–132.

[17] Weis J, Katona I, Müller-Newen G, Sommer C, Necula G, Hendrich C, *et al*. Small-fiber neuropathy in patients with ALS. Neurology. 2011; 76: 2024–2029.

[18] Li TM, Alberman E, Swash M. Comparison of sporadic and familial disease amongst 580 cases of motor neuron disease. Journal of Neurology, Neurosurgery & Psychiatry. 1988; 51: 778–784.

[19] Anagnostou E, Zachou A, Breza M, Kladi A, Karadima G, Koutsis G. Disentangling balance impairments in spinal and bulbar muscular atrophy. Neuroscience Letters. 2019; 705: 94–98.

[20] Li Hi Shing S, Chipika RH, Finegan E, Murray D, Hardiman O, Bede P. Post-polio Syndrome: more than Just a Lower Motor Neuron Disease. Frontiers in Neurology. 2019; 10: 773.

[21] Finegan E, Chipika RH, Li Hi Shing S, Doherty MA, Hengeveld JC, Vajda A, *et al*. The clinical and radiological profile of primary lateral sclerosis: a population-based study. Journal of Neurology. 2019; 266: 2718–2733.

[22] Pradat P, Bernard E, Corcia P, Couratier P, Jublanc C, Querin G, *et al*. The French national protocol for Kennedy's disease

(SBMA): consensus diagnostic and management recommendations. Orphanet Journal of Rare Diseases. 2020; 15: 90.
[23] Deepika J, Manvir B, Sumit S, Vinay G, Trilochan S, Garima S, *et al*. Quantitative thermal sensory testing in patients with amyotrophic lateral sclerosis using reaction time exclusive method of levels (MLE). Electroencephalography and Clinical Neurophysiology. 2006; 46: 145–148.
[24] Xu Y, Zhang J, Zheng J, Zhang S, Kang D, Fan D. Fully intact contact heat evoked potentials in patients with amyotrophic lateral sclerosis. Muscle & Nerve. 2009; 39: 735–738.
[25] Rabin BA, Griffin JW, Crain BJ, Scavina M, Chance PF, Cornblath DR. Autosomal dominant juvenile amyotrophic lateral sclerosis. Brain. 1999; 122: 1539–1550.
[26] Camu W, Khoris J, Moulard B, Salachas F, Briolotti V, Rouleau GA, *et al*. Genetics of familial ALS and consequences for diagnosis. French ALS Research Group. Journal of the Neurological Sciences. 1999; 165: S21–S26.
[27] Dyck PJ, Stevens JC, Mulder DW, Espinosa RE. Frequency of nerve fiber degeneration of peripheral motor and sensory neurons in amyotrophic lateral sclerosis. Morphometry of deep and superficial peroneal nerves. Neurology. 1975; 25: 781–785.
[28] Khoris J, Moulard B, Briolotti V, Hayer M, Durieux A, Clavelou P, *et al*. Coexistence of dominant and recessive familial amyotrophic lateral sclerosis with the D90a Cu,Zn superoxide dismutase mutation within the same country. European Journal of Neurology. 2000; 7: 207–211.
[29] Moisset X, Cornut-Chauvinc C, Clavelou P, Pereira B, Dallel R, Guy N. Is there pain with neuropathic characteristics in patients with amyotrophic lateral sclerosis? A cross-sectional study. Palliative Medicine. 2016; 30: 486–494.
[30] Lukomski M, Klimek A. Badanie elektronystagmograficzne u chorych z SLA [Electronystagmographic examination in patients with amyotrophic lateral sclerosis (ALS)]. Neurologia i Neurochirurgia Polska. 1993; 27: 493–498. (In Polish)
[31] Simmatis L, Atallah G, Scott SH, Taylor S. The feasibility of using robotic technology to quantify sensory, motor, and cognitive impairments associated with ALS. Amyotrophic Lateral Sclerosis and Frontotemporal Degeneration. 2019; 20: 43–52.
[32] Elian M. Olfactory impairment in motor neuron disease: a pilot study. Journal of Neurology, Neurosurgery, and Psychiatry. 1991; 54: 927–928.
[33] Hawkes CH, Shephard BC, Geddes JF, Body GD, Martin JE. Olfactory disorder in motor neuron disease. Experimental Neurology. 1998; 150: 248–253.
[34] Günther R, Schrempf W, Hähner A, Hummel T, Wolz M, Storch A, *et al*. Impairment in Respiratory Function Contributes to Olfactory Impairment in Amyotrophic Lateral Sclerosis. Frontiers in Neurology. 2018; 9: 79.
[35] Günther R, Richter N, Sauerbier A, Chaudhuri KR, Martinez-Martin P, Storch A, *et al*. Non-Motor Symptoms in Patients Suffering from Motor Neuron Diseases. Frontiers in Neurology. 2016; 7: 117.
[36] Tarlarini C, Greco LC, Lizio A, Gerardi F, Sansone VA, Lunetta C. Taste changes in amyotrophic lateral sclerosis and effects on quality of life. Neurological Sciences. 2019; 40: 399–404.
[37] Yunusova Y, Plowman EK, Green JR, Barnett C, Bede P. Clinical Measures of Bulbar Dysfunction in ALS. Frontiers in Neurology. 2019; 10: 106.
[38] Wagner ML, Landis BE. Riluzole: a new agent for amyotrophic lateral sclerosis. The Annals of Pharmacotherapy. 1997; 31: 738–744.
[39] Ruoppolo G, Onesti E, Gori MC, Schettino I, Frasca V, Biasiotta A, *et al*. Laryngeal Sensitivity in Patients with Amyotrophic Lateral Sclerosis. Frontiers in Neurology. 2016; 7: 212.
[40] Amin MR, Harris D, Cassel SG, Grimes E, Heiman-Patterson T. Sensory testing in the assessment of laryngeal sensation in patients with amyotrophic lateral sclerosis. The Annals of Otology, Rhinology, and Laryngology. 2006; 115: 528–534.
[41] Bede P, Querin G, Pradat P. The changing landscape of motor neuron disease imaging: the transition from descriptive studies to precision clinical tools. Current Opinion in Neurology. 2018; 31: 431–438.
[42] Behnia M, Kelly JJ. Role of electromyography in amyotrophic lateral sclerosis. Muscle & Nerve. 1991; 14: 1236–1241.
[43] Sangari S, Giron A, Marrelec G, Pradat P, Marchand-Pauvert V. Abnormal cortical brain integration of somatosensory afferents in ALS. Clinical Neurophysiology. 2018; 129: 874–884.
[44] Shimizu T, Bokuda K, Kimura H, Kamiyama T, Nakayama Y, Kawata A, *et al*. Sensory cortex hyperexcitability predicts short survival in amyotrophic lateral sclerosis. Neurology. 2018; 90: e1578–e1587.
[45] Isak B, Tankisi H, Johnsen B, Pugdahl K, Finnerup NB, Fuglsang-Frederiksen A. Laser and somatosensory evoked potentials in amyotrophic lateral sclerosis. Clinical Neurophysiology. 2016; 127: 3322–3328.
[46] Constantinovici A. Abnormal somatosensory evoked potentials in amyotrophic lateral sclerosis. Romanian Journal of Neurology and Psychiatry. 1993; 31: 273–278.
[47] Münte TF, Tröger MC, Nusser I, Wieringa BM, Johannes S, Matzke M, *et al*. Alteration of early components of the visual evoked potential in amyotrophic lateral sclerosis. Journal of Neurology. 1998; 245: 206–210.
[48] Matheson JK, Harrington HJ, Hallett M. Abnormalities of multimodality evoked potentials in amyotrophic lateral sclerosis. Archives of Neurology. 1986; 43: 338–340.
[49] Mondelli M, Rossi A, Passero S, Guazzi GC. Involvement of peripheral sensory fibers in amyotrophic lateral sclerosis: electrophysiological study of 64 cases. Muscle & Nerve. 1993; 16: 166–172.
[50] Jamal GA, Weir AI, Hansen S, Ballantyne JP. Sensory involvement in motor neuron disease: further evidence from automated thermal threshold determination. Journal of Neurology, Neurosurgery, and Psychiatry. 1985; 48: 906–910.
[51] Marjanović IV, Selak-Djokić B, Perić S, Janković M, Arsenijević V, Basta I, *et al*. Comparison of the clinical and cognitive features of genetically positive ALS patients from the largest tertiary center in Serbia. Journal of Neurology. 2017; 264: 1091–1098.
[52] Yoshizawa K, Yasuda N, Fukuda M, Yukimoto Y, Ogino M, Hata W, *et al*. Syntactic comprehension in patients with amyotrophic lateral sclerosis. Behavioural Neurology. 2014; 2014: 230578.
[53] Fatima M, Tan R, Halliday GM, Kril JJ. Spread of pathology in amyotrophic lateral sclerosis: assessment of phosphorylated TDP-43 along axonal pathways. Acta Neuropathologica Communications. 2015; 3: 47.
[54] Luigetti M, Conte A, Del Grande A, Bisogni G, Romano A, Sabatelli M. Sural nerve pathology in ALS patients: a single-centre experience. Neurological Sciences. 2012; 33: 1095–1099.
[55] Nagy D, Kato T, Kushner PD. Reactive astrocytes are widespread in the cortical gray matter of amyotrophic lateral sclerosis. Journal of Neuroscience Research. 1994; 38: 336–347.
[56] Geser F, Brandmeir NJ, Kwong LK, Martinez-Lage M, Elman L, McCluskey L, *et al*. Evidence of multisystem disorder in whole-brain map of pathological TDP-43 in amyotrophic lateral sclerosis. Archives of Neurology. 2008; 65: 636–641.
[57] Cohen-Adad J, El Mendili M, Morizot-Koutlidis R, Lehéricy S, Meininger V, Blancho S, *et al*. Involvement of spinal sensory pathway in ALS and specificity of cord atrophy to lower motor neuron degeneration. Amyotrophic Lateral Sclerosis & Frontotemporal Degeneration. 2013; 14: 30–38.

[58] Rasoanandrianina H, Grapperon A, Taso M, Girard OM, Duhamel G, Guye M, *et al*. Region-specific impairment of the cervical spinal cord (SC) in amyotrophic lateral sclerosis: a preliminary study using SC templates and quantitative MRI (diffusion tensor imaging/inhomogeneous magnetization transfer). NMR in Biomedicine. 2017; 30.

[59] Chipika RH, Finegan E, Li Hi Shing S, McKenna MC, Christidi F, Chang KM, *et al*. "Switchboard" malfunction in motor neuron diseases: Selective pathology of thalamic nuclei in amyotrophic lateral sclerosis and primary lateral sclerosis. NeuroImage: Clinical. 2020; 27: 102300.

[60] Chipika RH, Siah WF, Shing SLH, Finegan E, McKenna MC, Christidi F, *et al*. MRI data confirm the selective involvement of thalamic and amygdalar nuclei in amyotrophic lateral sclerosis and primary lateral sclerosis. Data in Brief. 2020; 32: 106246.

[61] Cosottini M, Pesaresi I, Piazza S, Diciotti S, Cecchi P, Fabbri S, *et al*. Structural and functional evaluation of cortical motor areas in Amyotrophic Lateral Sclerosis. Experimental Neurology. 2012; 234: 169–180.

[62] Grosskreutz J, Kaufmann J, Frädrich J, Dengler R, Heinze H, Peschel T. Widespread sensorimotor and frontal cortical atrophy in Amyotrophic Lateral Sclerosis. BMC Neurology. 2006; 6: 17.

[63] Bede P, Bokde A, Elamin M, Byrne S, McLaughlin RL, Jordan N, *et al*. Grey matter correlates of clinical variables in amyotrophic lateral sclerosis (ALS): a neuroimaging study of ALS motor phenotype heterogeneity and cortical focality. Journal of Neurology, Neurosurgery, and Psychiatry. 2013; 84: 766–773.

[64] Meoded A, Kwan JY, Peters TL, Huey ED, Danielian LE, Wiggs E, *et al*. Imaging findings associated with cognitive performance in primary lateral sclerosis and amyotrophic lateral sclerosis. Dementia and Geriatric Cognitive Disorders Extra. 2013; 3: 233–250.

[65] Abrahams S, Goldstein LH, Simmons A, Brammer M, Williams SCR, Giampietro V, *et al*. Word retrieval in amyotrophic lateral sclerosis: a functional magnetic resonance imaging study. Brain. 2004; 127: 1507–1517.

[66] Prell T, Hartung V, Tietz F, Penzlin S, Ilse B, Schweser F, *et al*. Susceptibility-weighted imaging provides insight into white matter damage in amyotrophic lateral sclerosis. PLoS ONE. 2015; 10: e0131114.

[67] Verma G, Woo JH, Chawla S, Wang S, Sheriff S, Elman LB, *et al*. Whole-brain analysis of amyotrophic lateral sclerosis by using echo-planar spectroscopic imaging. Radiology. 2013; 267: 851–857.

[68] Bede P, Iyer PM, Schuster C, Elamin M, Mclaughlin RL, Kenna K, *et al*. The selective anatomical vulnerability of ALS: 'disease-defining' and 'disease-defying' brain regions. Amyotrophic Lateral Sclerosis & Frontotemporal Degeneration. 2016; 17: 561–570.

[69] Verstraete E, Turner MR, Grosskreutz J, Filippi M, Benatar M. Mind the gap: the mismatch between clinical and imaging metrics in ALS. Amyotrophic Lateral Sclerosis & Frontotemporal Degeneration. 2015; 16: 524–529.

[70] Chipika RH, Christidi F, Finegan E, Li Hi Shing S, McKenna MC, Chang KM, *et al*. Amygdala pathology in amyotrophic lateral sclerosis and primary lateral sclerosis. Journal of the Neurological Sciences. 2020; 417: 117039.

[71] Fischl B. FreeSurfer. NeuroImage. 2012; 62: 774–781.

[72] Fischl B, Dale AM. Measuring the thickness of the human cerebral cortex from magnetic resonance images. Proceedings of the National Academy of Sciences of the United States of America. 2000; 97: 11050–11055.

[73] Iglesias JE, Insausti R, Lerma-Usabiaga G, Bocchetta M, Van Leemput K, Greve DN, *et al*. A probabilistic atlas of the human thalamic nuclei combining ex vivo MRI and histology. NeuroImage. 2018; 183: 314–326.

[74] Saygin ZM, Kliemann D, Iglesias JE, van der Kouwe AJW, Boyd E, Reuter M, *et al*. High-resolution magnetic resonance imaging reveals nuclei of the human amygdala: manual segmentation to automatic atlas. NeuroImage. 2017; 155: 370–382.

[75] Mori S, Oishi K, Jiang H, Jiang L, Li X, Akhter K, *et al*. Stereotaxic white matter atlas based on diffusion tensor imaging in an ICBM template. NeuroImage. 2008; 40: 570–582.

[76] Bede P, Chipika RH, Finegan E, Li Hi Shing S, Doherty MA, Hengeveld JC, *et al*. Brainstem pathology in amyotrophic lateral sclerosis and primary lateral sclerosis: a longitudinal neuroimaging study. NeuroImage: Clinical. 2019; 24: 102054.

[77] Burke T, Elamin M, Bede P, Pinto-Grau M, Lonergan K, Hardiman O, *et al*. Discordant performance on the 'Reading the Mind in the Eyes' Test, based on disease onset in amyotrophic lateral sclerosis. Amyotrophic Lateral Sclerosis & Frontotemporal Degeneration. 2016; 17: 467–472.

[78] Burke T, Pinto-Grau M, Lonergan K, Elamin M, Bede P, Costello E, *et al*. Measurement of Social Cognition in Amyotrophic Lateral Sclerosis: a Population Based Study. PLoS ONE. 2016; 11: e0160850.

[79] Abidi M, Marco G, Couillandre A, Feron M, Mseddi E, Termoz N, *et al*. Adaptive functional reorganization in amyotrophic lateral sclerosis: coexisting degenerative and compensatory changes. European Journal of Neurology. 2020; 27: 121–128.

[80] Feron M, Couillandre A, Mseddi E, Termoz N, Abidi M, Bardinet E, *et al*. Extrapyramidal deficits in ALS: a combined biomechanical and neuroimaging study. Journal of Neurology. 2018; 265: 2125–2136.

[81] Bede P, Omer T, Finegan E, Chipika RH, Iyer PM, Doherty MA, *et al*. Connectivity-based characterisation of subcortical grey matter pathology in frontotemporal dementia and ALS: a multimodal neuroimaging study. Brain Imaging and Behavior. 2018; 12: 1696–1707.

[82] Chipika RH, Finegan E, Li Hi Shing S, Hardiman O, Bede P. Tracking a Fast-Moving Disease: Longitudinal Markers, Monitoring, and Clinical Trial Endpoints in ALS. Frontiers in Neurology. 2019; 10: 229.

[83] Querin G, Bede P, El Mendili MM, Li M, Pélégrini-Issac M, Rinaldi D, *et al*. Presymptomatic spinal cord pathology in c9orf72 mutation carriers: A longitudinal neuroimaging study. Annals of Neurology. 2019; 86: 158–167.

[84] Müller H, Turner MR, Grosskreutz J, Abrahams S, Bede P, Govind V, *et al*. A large-scale multicentre cerebral diffusion tensor imaging study in amyotrophic lateral sclerosis. Journal of Neurology, Neurosurgery, and Psychiatry. 2016; 87: 570–579.

[85] Christidi F, Karavasilis E, Velonakis G, Ferentinos P, Rentzos M, Kelekis N, *et al*. The Clinical and Radiological Spectrum of Hippocampal Pathology in Amyotrophic Lateral Sclerosis. Frontiers in Neurology. 2018; 9:523.

[86] Pioro EP, Turner MR, Bede P. Neuroimaging in primary lateral sclerosis. Amyotrophic Lateral Sclerosis and Frontotemporal Degeneration. 2020; 21: 18–27.

[87] Finegan E, Li Hi Shing S, Chipika RH, Doherty MA, Hengeveld JC, Vajda A, *et al*. Widespread subcortical grey matter degeneration in primary lateral sclerosis: a multimodal imaging study with genetic profiling. NeuroImage: Clinical. 2019; 24: 102089.

[88] Finegan E, Hi Shing SL, Chipika RH, McKenna MC, Doherty MA, Hengeveld JC, *et al*. Thalamic, hippocampal and basal ganglia pathology in primary lateral sclerosis and amyotrophic lateral sclerosis: Evidence from quantitative imaging data. Data in Brief. 2020; 29: 105115.

[89] Rojas P, de Hoz R, Ramírez AI, Ferreras A, Salobrar-Garcia E, Muñoz-Blanco JL, *et al*. Changes in Retinal OCT and Their Correlations with Neurological Disability in Early ALS Patients, a Follow-Up Study. Brain Sciences. 2019; 9: 337.

[90] Bede P, Chipika RH, Christidi F, Hengeveld JC, Karavasilis E,

Argyropoulos GD, *et al*. Genotype-associated cerebellar profiles in ALS: focal cerebellar pathology and cerebro-cerebellar connectivity alterations. Journal of Neurology, Neurosurgery & Psychiatry. 2021; 92: 1197–1205.

[91] Christidi F, Karavasilis E, Rentzos M, Velonakis G, Zouvelou V, Xirou S, *et al*. Hippocampal pathology in amyotrophic lateral sclerosis: selective vulnerability of subfields and their associated projections. Neurobiology of Aging. 2019; 84: 178–188.

[92] Schuster C, Elamin M, Hardiman O, Bede P. The segmental diffusivity profile of amyotrophic lateral sclerosis associated white matter degeneration. European Journal of Neurology. 2016; 23: 1361–1371.

[93] Bede P, Chipika RH, Finegan E, Li Hi Shing S, Chang KM, Doherty MA, *et al*. Progressive brainstem pathology in motor neuron diseases: Imaging data from amyotrophic lateral sclerosis and primary lateral sclerosis. Data in Brief. 2020; 29: 105229.

[94] Abidi M, Marco G, Grami F, Termoz N, Couillandre A, Querin G, *et al*. Neural Correlates of Motor Imagery of Gait in Amyotrophic Lateral Sclerosis. Journal of Magnetic Resonance Imaging. 2021; 53: 223–233.

[95] Meier JM, Burgh HK, Nitert AD, Bede P, Lange SC, Hardiman O, *et al*. Connectome-Based Propagation Model in Amyotrophic Lateral Sclerosis. Annals of Neurology. 2020; 87: 725–738.

[96] Pelletier CA, Abou-Zeid E, Bartoshuk LM, Rudnicki SA. Is Taste Altered in Patients with ALS? Chemosensory Perception. 2013; 6: 101–107.

[97] Tahedl M, Li Hi Shing S, Finegan E, Chipika RH, Lope J, Hardiman O, *et al*. Propagation patterns in motor neuron diseases: Individual and phenotype-associated disease-burden trajectories across the UMN-LMN spectrum of MNDs. Neurobiology of Aging. 2021; 109: 78–87.

[98] El Mendili MM, Querin G, Bede P, Pradat P. Spinal Cord Imaging in Amyotrophic Lateral Sclerosis: Historical Concepts-Novel Techniques. Frontiers in Neurology. 2019; 10: 350.

[99] Bede P, Bokde AL, Byrne S, Elamin M, Fagan AJ, Hardiman O. Spinal cord markers in ALS: diagnostic and biomarker considerations. Amyotrophic Lateral Sclerosis. 2012; 13: 407–415.